Available online at www.sciencedirect.com
SCIENCE DIRECT®
Remote Sensing of Environment 90 (2004) 463–476
Remote Sensing of Environment
www.elsevier.com/locate/rse

Hyperspectral indices and model simulation for chlorophyll estimation in open-canopy tree crops

P.J. Zarco-Tejada[a,*], J.R. Miller[b], A. Morales[c], A. Berjón[a], J. Agüera[d]

[a] *GOA-UVA, Universidad de Valladolid, Valladolid, Spain*
[b] *Department of Physics and Astronomy, York University, Toronto, Canada*
[c] *Departamento de Ciencias Agroforestales, Universidad de Sevilla, Sevilla, Spain*
[d] *Departamento de Ingeniería Rural, Universidad de Córdoba, Córdoba, Spain*

Received 24 June 2003; received in revised form 21 January 2004; accepted 22 January 2004

Abstract

An investigation of the estimation of leaf biochemistry in open tree crop canopies using high-spatial hyperspectral remote sensing imagery is presented. Hyperspectral optical indices related to leaf chlorophyll content were used to test different radiative transfer modelling assumptions in open canopies where crown, soil and shadow components were separately targeted using 1 m spatial resolution ROSIS hyperspectral imagery. Methods for *scaling-up* of hyperspectral single-ratio indices such as R_{750}/R_{710} and combined indices such as MCARI, TCARI and OSAVI were studied to investigate the effects of scene components on indices calculated from pure crown pixels and from aggregated soil, shadow and crown reflectance. Methods were tested on 1-m resolution hyperspectral ROSIS datasets acquired over two olive groves in southern Spain during the HySens 2002 campaign conducted by the German Aerospace Center (DLR). Leaf-level biochemical estimation using 1-m ROSIS data when targeting pure olive tree crowns employed PROSPECT-SAILH radiative transfer simulation. At lower spatial resolution, therefore with significant effects of soil and shadow scene components on the aggregated pixels, a canopy model to account for such scene components had to be used for a more appropriate estimation approach for leaf biochemical concentration. The linked models PROSPECT-SAILH-FLIM improved the estimates of chlorophyll concentration from these open tree canopies, demonstrating that crown-derived relationships between hyperspectral indices and biochemical constituents cannot be readily applied to hyperspectral imagery of lower spatial resolutions due to large soil and shadow effects. Predictive equations built on a MCARI/OSAVI *scaled-up* index through radiative transfer simulation minimized soil background variations in these open canopies, demonstrating superior performance compared to other single-ratio indices previously shown as good indicators of chlorophyll concentration in closed canopies. The MCARI/OSAVI index was demonstrated to be less affected than TCARI/OSAVI by soil background variations when calculated from the pure crown component even at the typically low LAI orchard and grove canopies.

Keywords: Chlorophyll content; Open canopy; Hyperspectral; Remote sensing; Radiative transfer; Olive tree; FLIM

1. Introduction

The estimation of leaf biochemistry in high-value crops such as *Olea europaea* L., *Vitis vinifera* L. and orchard tree crops have important potential implications for agricultural field management, crop stress and chlorosis detection, and especially for precision agriculture practices. Chlorophyll concentration (C_{ab}) and other leaf biochemical constituents, such as dry matter (C_m) and water content (C_w) may be used as indicators of crop stress through their potential influence on nutritional deficiencies (Chen & Barak, 1982; Fernández-Escobar et al., 1999; Jolley & Brown, 1994; Marschner et al., 1986; Tagliavini & Rombolà, 2001; Wallace, 1991). Such deficiencies may be related to crop chlorosis that can be successfully treated thereby improving yields and the final crop quality (Chova et al., 2000; Cordeiro et al., 1995; Fernández-Escobar et al., 1993; Gutiérrez-Rosales et al., 1992). On the other hand, over-fertilization of crops affects carbon storage, generates vegetation injury for prolonged N additions (Schulze et al., 1989) and increases N losses by gaseous and solute pathways to the soil. The total chlorophyll content in leaves decreases in stressed vegetation,

* Corresponding author. Current address: Instituto de Agricultura Sostenible (IAS), Consejo Superior de Investigaciones Científicas (CSIC), Apdo. de Correos 4084 14080, Córdoba, Spain. Tel.: +34-979-108414; fax: +34-979-108302.
E-mail address: pzarco@cica.es (P.J. Zarco-Tejada).

0034-4257/$ - see front matter © 2004 Elsevier Inc. All rights reserved.
doi:10.1016/j.rse.2004.01.017

changing the proportion of light-absorbing pigments and leading to less overall absorption due to lower chlorophyll *a* and *b* concentrations at the leaf level. Differences in reflectance between healthy and stressed vegetation due to changes in pigment content have been detected in the reflectance *green peak* and along the *red edge* (e.g. Carter, 1994; Gitelson & Merzlyak, 1996; Rock et al., 1988; Vogelmann et al., 1993), providing remote detection methods to map vegetation stress through the influence of chlorophyll content variation.

Several narrow-band leaf-level optical indices have been suggested for C_{ab} estimation from hyperspectral reflectance data (see Zarco-Tejada et al., 2001). Red Edge Reflectance Indices such as Vogelmann (R_{740}/R_{720}) and $(R_{734}-R_{747})/(R_{715}+R_{726})$; Gitelson and Merzlyak (R_{750}/R_{700}); Carter (R_{695}/R_{760}); Zarco-Tejada and Miller (R_{750}/R_{710}), and Spectral and Derivative Indices such as the red edge parameters λ_p, λ_o, σ (Miller et al., 1990), and derivative indices (D_{715}/D_{705}) and DP21 ($D\lambda_p/D_{703}$) have been shown to yield the best results for C_{ab} estimation at both leaf and canopy levels. Recently, combinations of indices based on TCARI, MCARI, and OSAVI, such as TCARI/OSAVI and MCARI/OSAVI (Haboudane et al., 2002), have been demonstrated to successfully minimize the effects of soil background

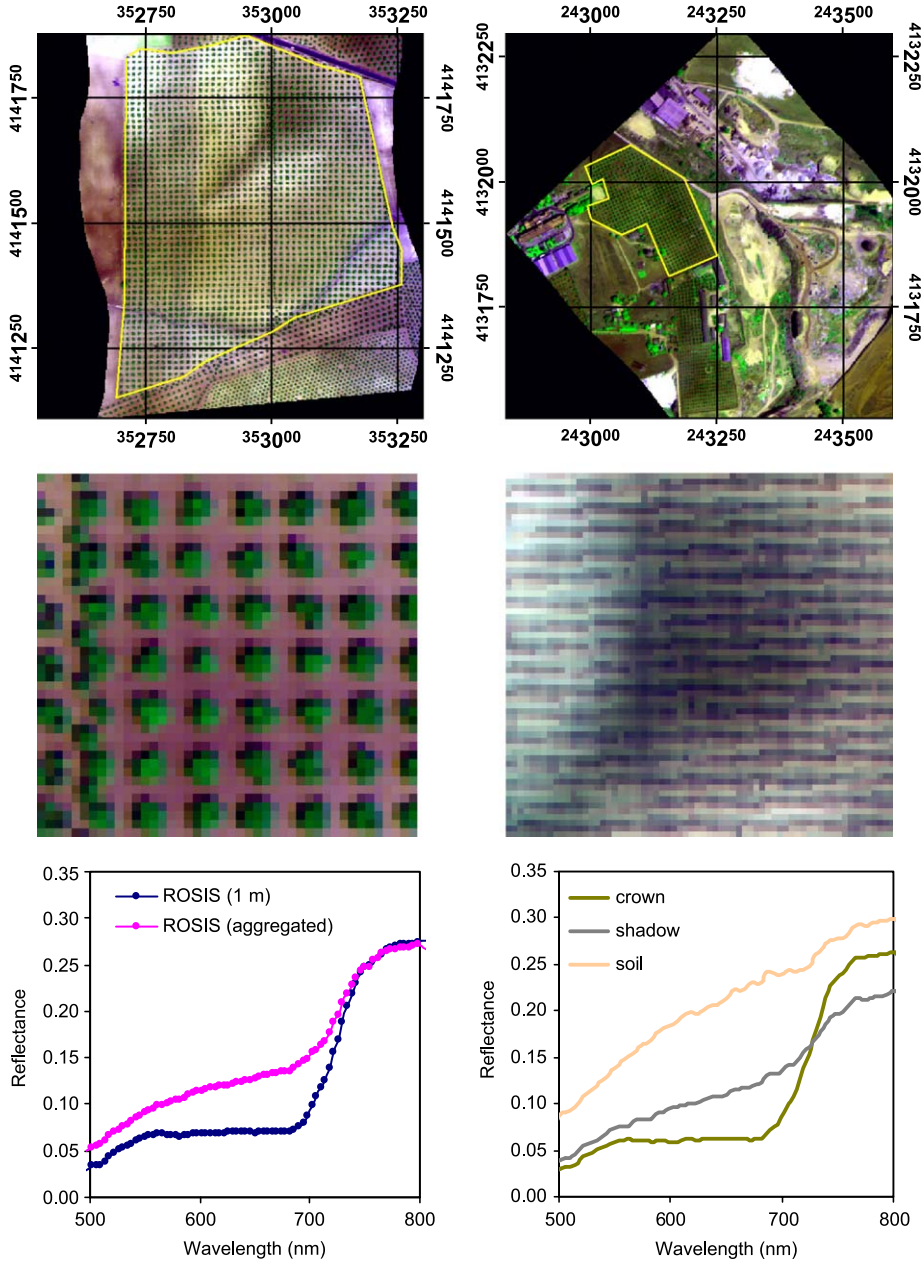

Fig. 1. ROSIS imagery collected at 1 m spatial resolution from the study fields of *Olea europaea* L. used in this study (top left and right). Imagery shows the crowns (middle left) and aggregated pixels (middle right) used for the modelling methods. Plots show the effect of scene components as function of the pixel size for ROSIS (lower left) and the crown, shadow and soil components (lower right).

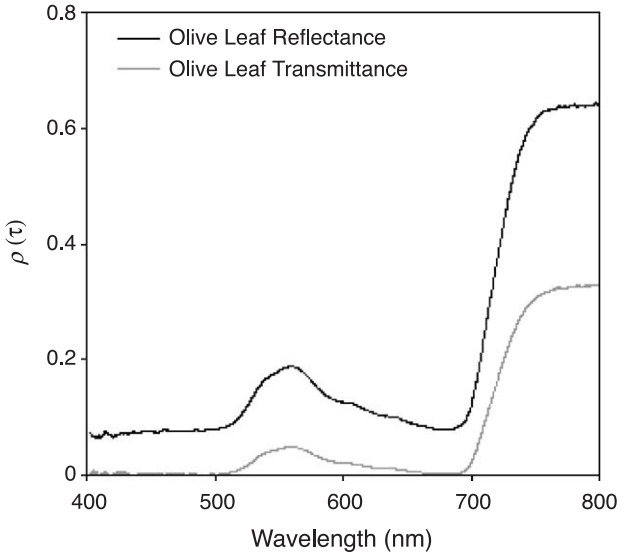

Fig. 2. Olive leaf reflectance (ρ) and transmittance (τ) measurements collected with a Li-Cor 1800-12 Integrating Sphere coupled to an Ocean Optics model USB2000 spectrometer.

variation and LAI canopy changes, resulting in prediction relationships for easy use for precision agriculture with *Compact Airborne Spectrographic Imager* (CASI) hyperspectral imagery.

The successful estimation of leaf biochemical constituents from hyperspectral data in homogeneous crops (Haboudane et al., 2002) and closed forest canopies (Zarco-Tejada et al., 2001) has demonstrated the utility of *scaled-up* indices through radiative transfer simulation. Moreover, model inversion techniques, based on linked leaf-canopy radiative transfer models, have been shown to be a feasible method for biochemical estimation from canopy-level reflectance in closed canopies (Jacquemoud, 1993; Jacquemoud et al., 1995, 2000) and through simulation studies modelling 3D forest canopies (Demarez & Gastellu-Etchegorry, 2000).

Nevertheless, and despite the successful results for C_{ab} estimation in closed canopies, estimation of leaf biochemistry in open crop canopies from remote sensing data requires appropriate modelling strategies which account for soil background and shadows which dominate the bidirectional reflectance (BRDF) signature. Reports of efforts to model the radiation interception by open crop canopies has been carried out by Villalobos et al. (1995) and Mariscal et al. (2000), although no further application of these radiative transfer methods on hyperspectral remote sensing data has been conducted.

The absence of successful estimation of leaf biochemistry from remote sensing for open crop canopies is presumably due to the difficulties to access suitable image data from hyperspectral sensors and to the complexity of the physical approaches required for modelling such canopies.

Research presented in this manuscript was conducted under the European Union HySens-2002 project designed to investigate physical methods to estimate leaf biochemical constituents in open crop canopies with the *Reflective Optics System Imaging Spectrometer* (ROSIS) high-spatial hyperspectral remote sensing imagery. Radiative transfer model assumptions for open canopies along with optimum hyperspectral optical indices for C_{ab} estimation need careful exploration. The application of optical indices in discontinuous crop canopies such as *Olea europaea* L., where canopy structure plays an important role, and the effect of LAI, shadows and soil in the modelled reflectance need extensive study with airborne hyperspectral data of optimum spatial and spectral resolution. Groves of *Olea europaea* L., grown in regular patterns with tree spacing typically between 6 and 12 m, were selected to study the associated dominant effects

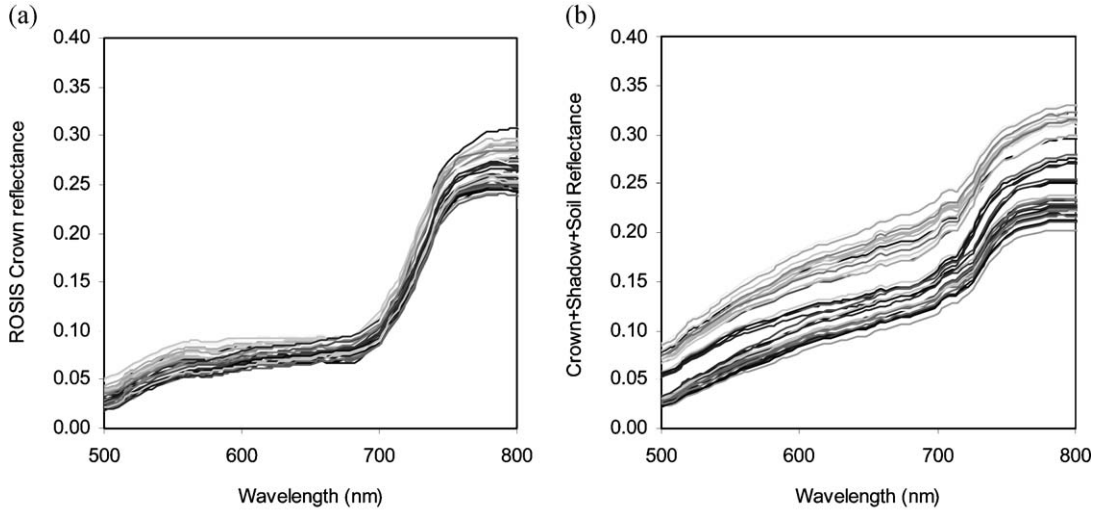

Fig. 3. Pure crown reflectance extracted from ROSIS imagery (a) and ROSIS aggregated spectra from soil, shadow and crowns (b) extracted from the trees selected for leaf sampling.

of soil and shadows on the canopy reflectance, employing appropriate radiative transfer simulation through leaf and canopy modelling.

2. ROSIS and DAIS airborne acquisitions and field data collection

An airborne campaign was conducted in Spain in July 2002 by the German Aerospace Center (DLR) with ROSIS and *Digital Airborne Imaging Spectrometer* (DAIS) sensors as part of the 2002 HySens campaigns. ROSIS imagery were acquired at 1 m spatial resolution from open-canopy crop fields of *Olea europaea* L. located in Córdoba and Seville regions of southern Spain (Fig. 1). Imagery was processed to *at-sensor* radiance at DLR, and atmospheric correction performed with MODTRAN using the aerosol optical depth at 550 nm collected with a Micro-Tops II sunphotometer (Solar Light, Philadelphia, PA, USA) at the time of airborne acquisition. Soil reflectance spectra were used to perform a *flat-field* correction (Ben-Dor & Levin, 2000) that compensated for residual effects on derived surface reflectance estimations in atmospheric water and oxygen absorption spectral regions.

A field sampling campaign was conducted for biochemical analysis of leaf C_{ab} at the tree level. Two fields of olive trees in southern Spain were selected to define a gradient in biochemical concentration, comprising groves of irrigated and non-irrigated crops. Differences in biochemical properties at the irrigated field corresponded to a random experimental study conducted with four fertirrigation treatments, with six blocks per treatment, and four trees per block. Treatments consisted on drip irrigation with water and no fertilizer, and 200, 400 and 600 g N per tree/irrigation with NPK fertilization 4:1:3. Reflectance (ρ) and transmittance (τ) measurements of olive leaves from treatment bocks were carried out with a Li-Cor 1800-12 Integrating Sphere (Li-Cor, Lincoln, NE, USA), coupled by a 200 μm diameter single mode fiber to an Ocean Optics model USB2000 spectrometer (Ocean Optics, Dunedin, FL, USA), with a 1024 element detector array, 0.5 nm sampling interval, and 7.5 nm spectral resolution in the 340–940 nm range. A leaf-level measurement protocol used for leaf reflectance and transmittance was based on the methodology of Harron (2000), using a custom-made port of 0.5 cm diameter suited to typical olive leaf dimensions and thereby obtaining the leaf optical properties (Fig. 2).

A total of 552 leaves were sampled from 46 trees from the irrigated and non-irrigated fields. The 12 leaves per tree were sampled around the crown, placed in bags and stored at −23 °C prior to analysis. Two 2.3 cm circle samples were cut out of each leaf. One circle was ground into liquid N_2, weighed, and placed in a 15 ml centrifuge tube. The second circle was weighed, oven-dried at 80 °C for 24 h, and re-weighed. Ten milliliters of *N*,*N*-dimethylformamide (Spectralanalyzed grade, Fisher) was added to the tube, and 3 ml of supernatant was placed in a cuvette and the absorbance measured at 663.8, 646.8 and 480 nm with a Cary 1 spectrophotometer. Chlorophyll *a*, chlorophyll *b*, and total carotenoid concentrations were calculated using the extinction coefficients derived by Wellburn (1994), obtaining a mean C_{ab} and standard deviation from the sampled leaves of $\mu = 59.98$ μg/cm^2, $\sigma = 9.22$ ($n = 46$). Mean and standard deviation values for C_m were $\mu = 0.025$ mg/cm^2, $\sigma = 0.009$ ($n = 46$).

Additional field measurements made at the sites consisted of soil reflectance, shadow reflectance relative to above canopy irradiance, and crown transmittance derived using measurements with a diffuse cosine receptor within tree-crown shadow and under direct sun. Sampled trees were located in the 1 m resolution ROSIS image data, extracting reflectance from each tree separating the pure crown reflectance, direct soil and shadow reflectance (Fig. 3a). A second set of reflectance spectra were extracted from the ROSIS imagery, aggregating pixels around the crown, therefore obtaining a mixed signature of crown, soil and shadows (Fig. 3b). This second set of reflectance data from degraded resolution ROSIS imagery enabled the study of different modelling assumptions as function of pure crowns as compared to aggregation of the different scene components in these open canopies.

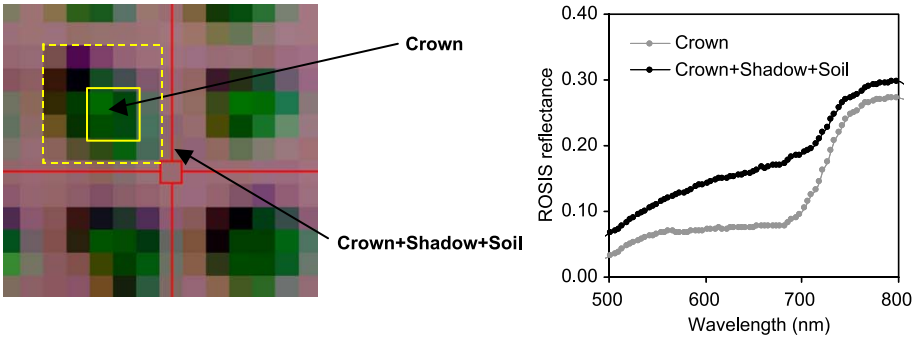

Fig. 4. Effects of scene component aggregation as function of pixels size, targeting the pure crown and when soil and shadows are averaged. Aggregation was conducted with a window of 5 × 5 pixels (25 pixels), including shadow and direct soil components. Pure crowns were selected with a 2 × 2 pixel window (4 pixels) including only pure vegetation.

3. Methods

The use of appropriate optical indices and radiative transfer simulation in open crop canopies are described in this section. Hyperspectral indices, that were previously demonstrated to estimate C_{ab} in forest and agricultural closed canopies, are tested for potential application to the open tree crop canopies in this study. *Scaling-up* approaches of such indices through different simulations and spatial resolutions are discussed in the following sections.

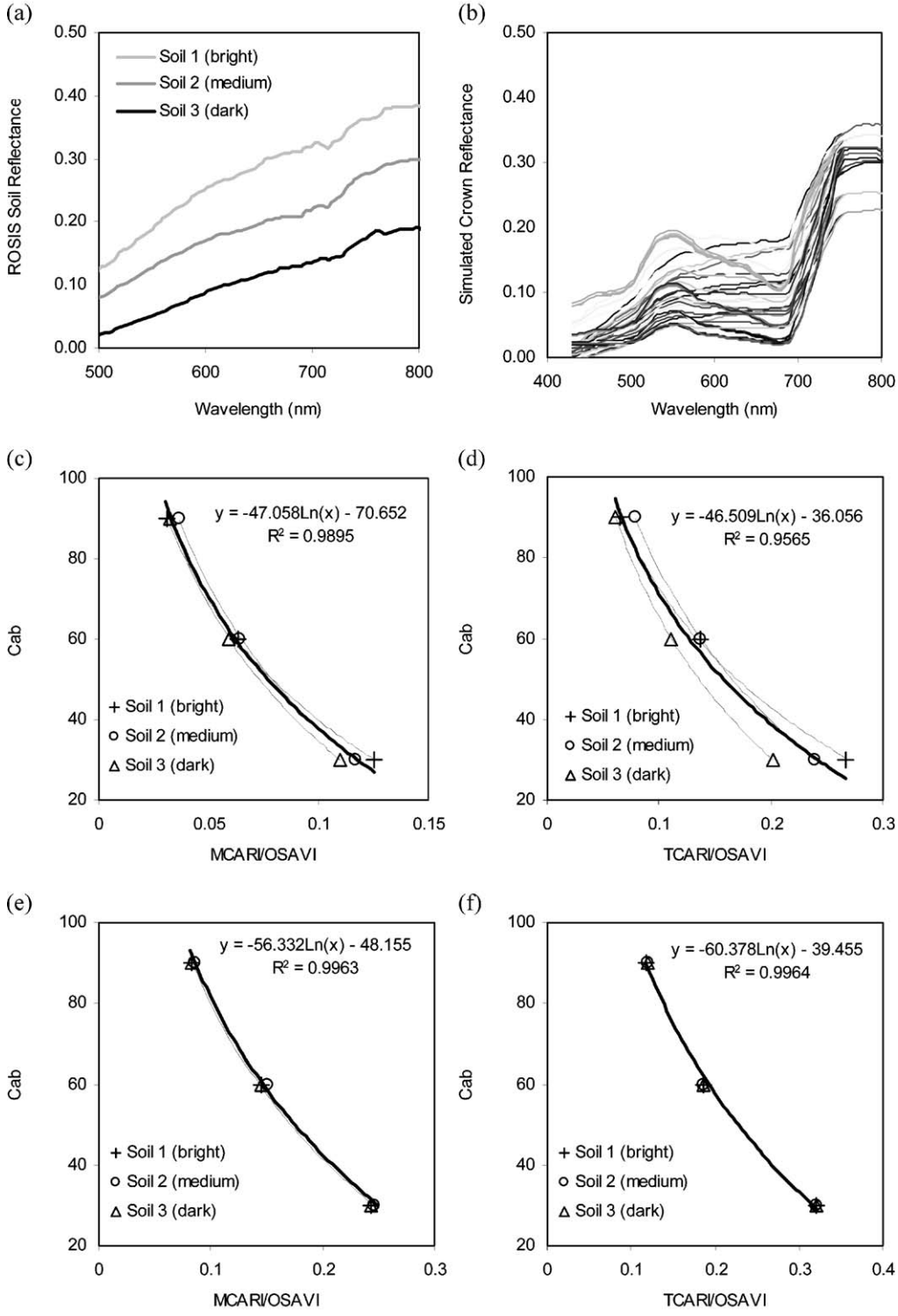

Fig. 5. Extreme values of soil reflectance used for the simulation (a). Simulated crown reflectance using PROSPECT-SAILH for a range of C_{ab} values (b). Relationship between MCARI/OSAVI (c,e) and TCARI/OSAVI (d,f) and C_{ab} as function of soil background (a) for LAI = 0.5 (c,d) and LAI = 3 (e,f).

3.1. Single ratio and combined optical indices for C_{ab} estimation

The *scaling-up* of optical indices through infinite reflectance models and radiative transfer simulation has been demonstrated in the past to successfully estimate leaf biochemistry from canopy-level reflectance in closed forest canopies (Zarco-Tejada et al., 2001) and homogeneous agricultural crops (Haboudane et al., 2002). Several indices have been proposed in the literature to track chlorophyll concentration, although such indices do not show the same performance at the leaf and at the canopy levels, due to the effects of scene components, soil and shadows, on canopy-level indices. Generally good results are found for C_{ab} estimation at the leaf level with *red edge* and spectral and derivative indices such as R_{750}/R_{710}, R_{740}/R_{720}, $(R_{734}-R_{747})/(R_{715}+R_{726})$, $(R_{734}-R_{747})/(R_{715}+R_{720})$, D_{715}/D_{705}, R_{750}/R_{550}, R_{750}/R_{700}, R_{695}/R_{760}, λ_p, $D\lambda_p/D_{703}$, and $D\lambda_p/D_{720}$ (Carter, 1994; Gitelson & Merzlyak, 1997; Vogelmann et al., 1993; Zarco-Tejada et al., 2001). Nevertheless, not all the previous leaf-level indices are successfully applied at the canopy level due to such canopy structural effects. Indices such as *red-edge* and spectral and derivative indices R_{750}/R_{710}, R_{740}/R_{720}, R_{750}/R_{700}, $(R_{734}-R_{747})/(R_{715}+R_{720})$, $(R_{734}-R_{747})/(R_{715}+R_{726})$, D_{715}/D_{705}, R_{750}/R_{550}, and R_{695}/R_{760} were shown to be the best indicators for C_{ab} estimation at both leaf and canopy levels.

These hyperspectral indices were successfully tested on closed canopies with potentially large shadow effects and small influences of soil background, demonstrating insensitivity to the influence of shadows (Zarco-Tejada et al., 2001). On the other hand, in agricultural canopies, with large effects of soil background and LAI variation at different growth stages, combined indices have been proposed to minimize such background soil effects while maximizing the sensitivity to C_{ab}. CARI (*Chlorophyll Absorption in Reflectance Index*) (Kim et al., 1994) was shown to reduce the variability of photosynthetically active radiation due to non-photosynthetic materials. MCARI (*Modified Chlorophyll Absorption in Reflectance Index*) (Daughtry et al., 2000) was a modification of CARI to minimize the combined effects of the soil reflectance and

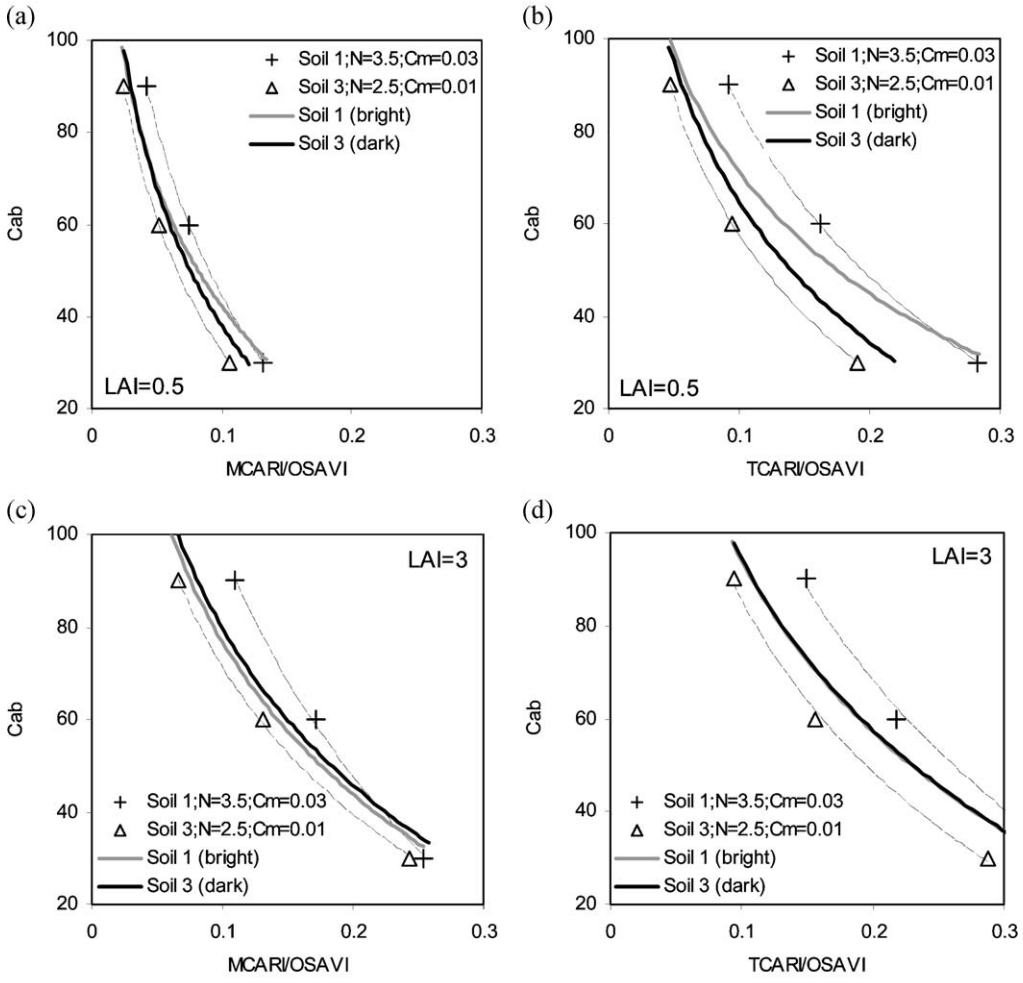

Fig. 6. Effects of leaf biochemical constituent C_m and leaf structure (N from PROSPECT) on MCARI/OSAVI (a,c) and TCARI/OSAVI (b,d) as function of C_{ab} (30 to 90 μg/cm^2), LAI (LAI = 0.5 in a,b; LAI = 3 in c,d), and soil background (bright and dark soil background).

the non-photosynthetic materials. SAVI (*Soil-Adjusted Vegetation Index*) (Huete, 1988) and OSAVI (*Optimized Soil-Adjusted Vegetation Index*) (Rondeaux et al., 1996) were proposed as soil-line vegetation indices that could be combined with MCARI to reduce background reflectance contributions (Daughtry et al., 2000). Successful C_{ab} estimation on corn agricultural canopies at different growing stages was achieved with the TCARI/OSAVI combined index, proving its robustness in the presence of variations in canopy LAI and background exposure (Haboudane et al., 2002).

The superior performance of combined optical indices over single ratios for minimizing background reflectance was tested in the open crop canopies, the subject of this study. Crown reflectance spectra extracted from the trees used for field sampling (Fig. 3a) and from the aggregated pixels containing pure crown vegetation, soil, and shadow (Fig. 3b) were used to calculate the red edge single ratio index R_{750}/R_{710}, and MCARI, TCARI, OSAVI, MCARI/OSAVI and TCARI/OSAVI combined indices, determining the relationships with ground-measured C_{ab} content.

3.2. Scaling-up methods for open crop canopies with SAILH and FLIM models

Single-ratio and combined indices described in the previous section were *scaled up* through radiative transfer simulation linking PROSPECT leaf model (Jacquemoud & Baret, 1990) with SAILH canopy model (Verhoef, 1984) and the *Forest Light Interaction Model* (FLIM) (Rosema et al., 1992). The objective here was to study the influence of scene components such as soil background, shadows, and crown reflectance on the estimation of C_{ab} biochemical constituent. The high spatial resolution of ROSIS imagery enabled the separation of scene components that could be used for the simulation through different canopy modelling assumptions (Fig. 4). FLIM uses a first-order approximation of stand reflectance, taking into account the effects of crown transparency on apparent reflectance of shadowed soil background. The canopy is considered as a discontinuous canopy layer with crowns and gaps, with primary variability in stand reflectance due to variations in crown coverage, shadows, and crown transmittance.

The set of reflectance spectra collected from pure crowns (Fig. 3a) was used for the simulation with PROSPECT-SAILH models and deriving predictive relationships as in Haboudane et al. (2002). The hypothesis considered was that SAILH model is valid for canopy simulation in open tree fields when the spatial resolution enables targeting the pure crown component. This assumption was tested, comparing C_{ab} estimated from PROSPECT-SAILH *scaled-up* indices with field-measured C_{ab} at the crown level. *Scaling up* method in these open canopies was conducted simulating canopy-level (crown) reflectance with PROSPECT-SAILH for a range of C_{ab} and extreme soil values, ranging from dark to bright soil reflectance (Fig. 5a) observed in scene pixels. Leaf-level spectra were simulated with PROSPECT parameter $N=3$ as derived from inversions of leaf-level optical measurements of field samples, with C_{ab} ranging from 20 to 90 μg/cm^2, and C_m and C_w fixed to 0.025 mg/

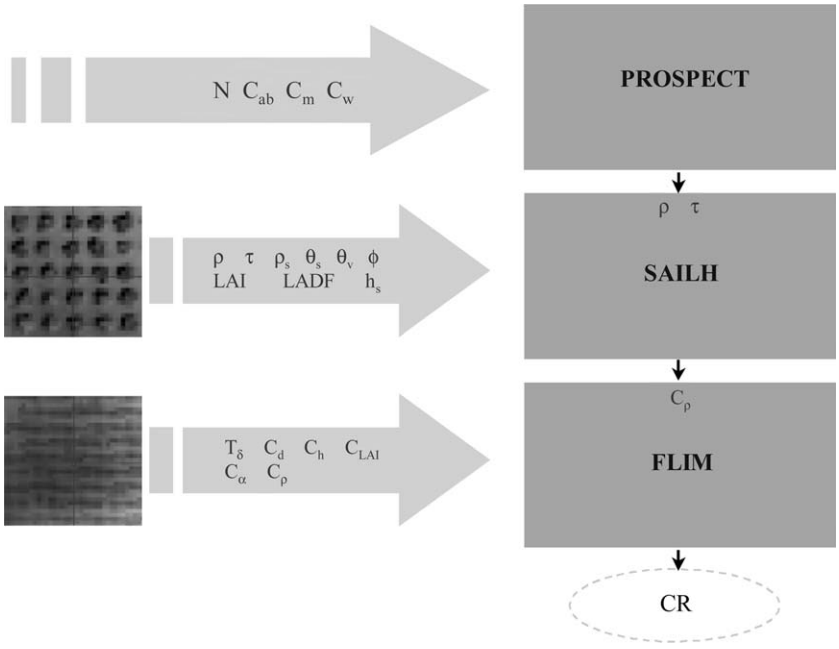

Fig. 7. Schematic view of the link between PROSPECT, SAILH and FLIM models, showing the input variables used for the simulation: leaf structural parameter N from PROSPECT, chlorophyll $a+b$ (C_{ab}), dry matter (C_m), equivalent water thickness (C_w), leaf reflectance and transmittance (ρ, τ), soil reflectance (ρ_s), viewing geometry θ_s,θ_v,ϕ, canopy LAI, leaf angle distribution function (LADF), hotspot (h_s), tree density (T_δ), crown diameter (C_d), crown height (C_h), crown LAI (C_{LAI}), crown extinction coefficient (C_α), and crown reflectance (C_ρ).

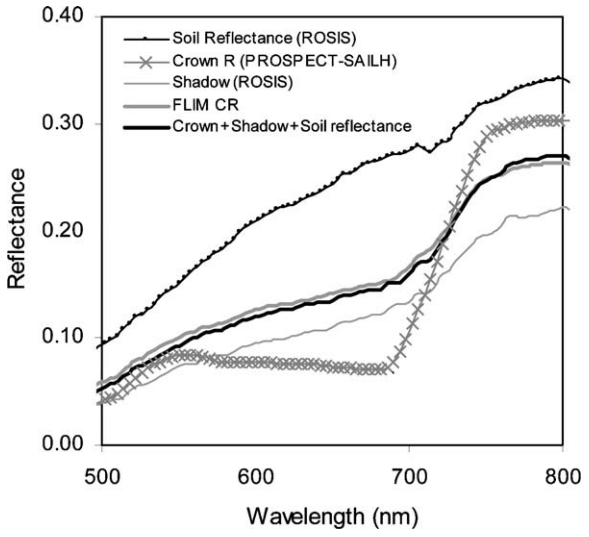

Fig. 8. Canopy reflectance simulation with PROSPECT-SAILH-FLIM obtained for $T_\delta = 200$ trees/ha, $C_d = 7$ m, $C_h = 3$ m, $C_{LAI} = 1$, $C_\alpha = 0.6$, $\theta_s = 40°$, ρ_s obtained from imagery, and crown reflectance ρ_c from SAILH.

cm^2. SAILH input parameters comprised of LAI ranging from 0.5 to 6, plagiophile leaf angle distribution function, the viewing geometry at the time of the airborne acquisition (θ_s, θ_v, ϕ) and three soil reflectance spectra collected from the imagery representing extreme values. Simulated spectra with PROSPECT-SAILH (Fig. 5b) were used to calculate single-ratio and combined indices described in the previous section to derive relationships with C_{ab}. These relationships show the sensitivity of C_{ab} variation on combined indices such as MCARI/OSAVI (Fig. 5c,e) and TCARI/OSAVI (Fig. 5d,f) for different soil backgrounds and low LAI values (LAI = 0.5, Fig. 5c,d), indicating that larger effects due to variations in soil background for low LAI are found on TCARI/OSAVI compared to the MCARI/OSAVI index. At larger LAI values (LAI = 3, Fig. 5e,f) no effects are found on either combined index TCARI/OSAVI or MCARI/OSAVI as function of soil backgrounds.

The effects of the leaf biochemical constituent C_m and leaf structure on combined indices as function of C_{ab}, LAI and soil background were also studied (Fig. 6). Indices MCARI/OSAVI and TCARI/OSAVI calculated with fixed

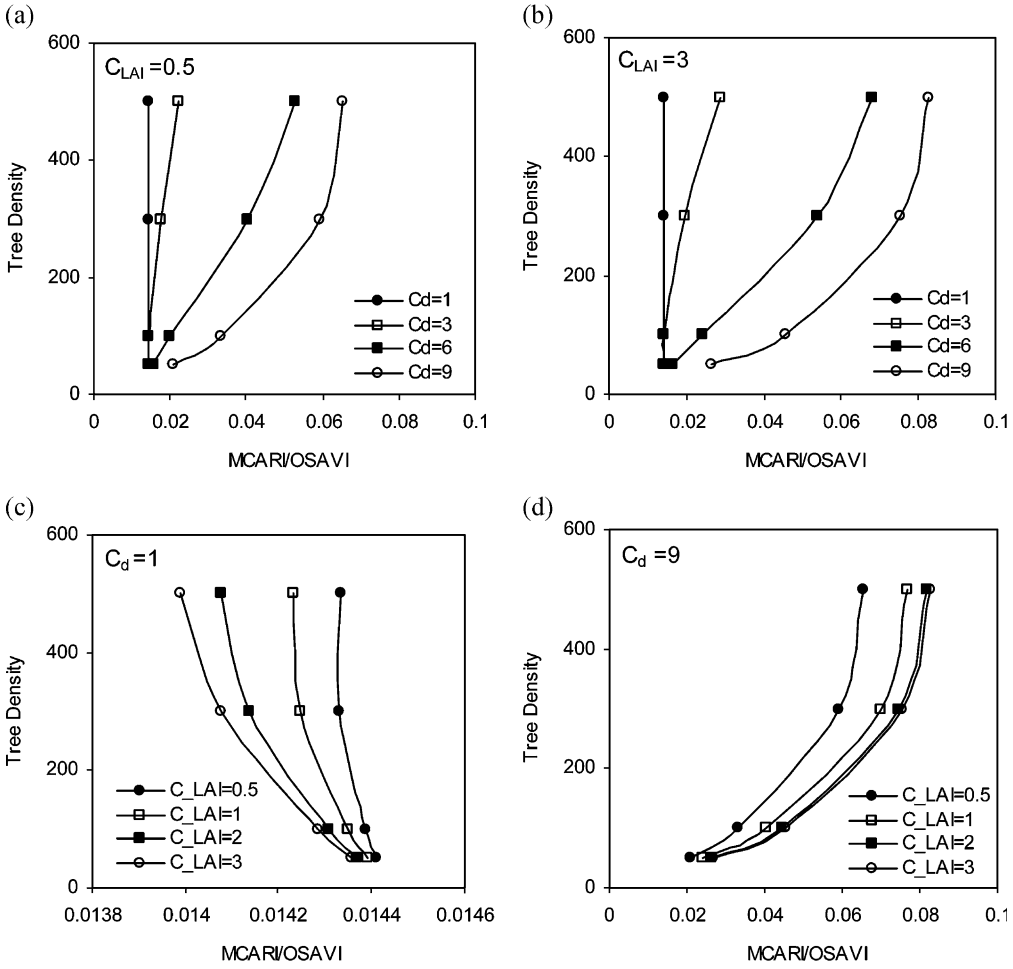

Fig. 9. Effects of FLIM geometrical variables tree density, T_δ, crown diameter, C_d, and crown leaf area, C_{LAI} on MCARI/OSAVI index. MCARI/OSAVI was simulated as function of T_δ (ranging between 50 and 500 trees/ha) for C_d between 1 and 9 m, and C_{LAI} between 0.5 and 3.

Table 1
Nominal values and range of parameters used for leaf and canopy modelling with PROSPECT, SAILH and FLIM for olive-tree study sites

Canopy structural parameters	Nominal values and range
Tree density (T_δ)	50–500 trees/ha
Crown diameter (C_d)	1–9 m
Crown height (C_h)	3 m
Crown leaf area (C_{LAI})	0.5–3 m
Crown parameters	**Nominal values**
Crown extinction coefficient (C_α)	0.6
Leaf angle distribution (LADF)	Plagiophile
Background and viewing geometry	**Nominal values**
Soil reflectance (ρ_s)	from image, Soil 2 (Fig. 5)
Leaf angle distribution (LADF)	Plagiophile
Viewing geometry ($\theta_s\theta_v\phi$)	$\theta_s = 30°$, $\theta_v = 0°$, $\phi = 0°$
Leaf parameters	**Nominal values**
Chlorophyll $a+b$ (C_{ab})	60 μg/cm^2
Dry matter (C_m)	0.025 mg/cm^2
Equivalent water thickness (C_w)	0.025 mg/cm^2
Structural parameter (N)	2.9

Canopy structural parameters were used in the FLIM model for simulation of the canopy reflectance by radiative transfer. Leaf structural parameters, and leaf biochemical parameters were used for leaf-level simulation of reflectance and transmittance using PROSPECT.

values of C_m (0.025 mg/cm^2) and N (3) for bright (soil 1) and dark (soil 3) soil background (Fig. 6, solid lines) were also calculated with olive-leaf typical range of variation for N (ranging from 2.5 to 3.5) and C_m (0.01–0.03 mg/cm^2). MCARI/OSAVI calculated as function of C_{ab} (Fig. 6a,c) and TCARI/OSAVI (Fig. 6b,d) for LAI = 0.5 (Fig. 6a,b) and LAI = 3 (Fig. 6c,d) show that C_m and N effects on the combined indices are smaller for MCARI/OSAVI than for TCARI/OSAVI. Nevertheless, simulations show that such leaf variables should be carefully considered when using

Table 2
Determination coefficients obtained between optical indices and ground measured C_{ab}

Index	Targeting crowns	Aggregated pixels
R_{750}/R_{710}	0.07	0.14
TCARI	0.6	0.3
MCARI	0.64	0.27
OSAVI	0.09	0.08
TCARI/OSAVI	0.48	0.32
MCARI/OSAVI	0.69	0.35

MCARI/OSAVI index for C_{ab} estimation. The confounding effects of a dark soil, lower N (2.5) and lower C_m (0.01) compared with the index simulated with the opposite, with brighter soil, higher N (3.5) and higher C_m (0.03) could potentially introduce an error on C_{ab} estimation of up to 15 μg/cm^2, depending on LAI and C_{ab} ranges.

The set of reflectance spectra collected from the aggregated pixels, including crown, shadow and soil components (Figs. 3b and 4) was used to study their effects on the indices used for C_{ab} estimation. Moreover, it allowed us to test different radiative transfer simulations for correct estimation of C_{ab} by scaling up the optical indices. This is particularly important for sensors with lower spatial resolutions, therefore acquiring data with pixels comprised of an aggregation of soil, shadow and crown components. In this case, the modelling method consisted of linking SAILH and FLIM models (PROSPECT-SAILH-FLIM), as SAILH simulates the crown reflectance, while FLIM simulates the geometry of the open canopy, including the effects of vegetation crowns, and sunlit and shadowed background soil (Fig. 7). The FLIM model input variables are tree density (T_δ), crown diameter (C_d), crown height (C_h) and crown leaf area (C_{LAI}), crown extinction coefficient (C_α), sun angle (θ_s), background reflectance (ρ_s), obtaining crown reflectance (ρ_c) from SAILH. Fig. 8 shows a best-fit simulation from PROS-

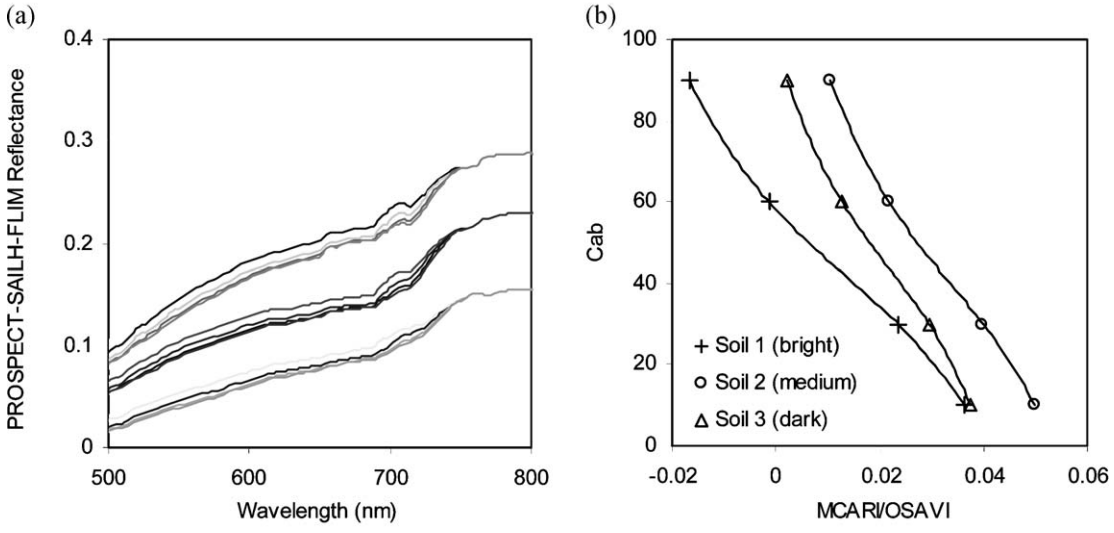

Fig. 10. PROSPECT-SAILH-FLIM simulation generating a set of spectra for different C_{ab} values (C_{ab} = 10, 30, 60 and 90 μg/cm^2) and soil backgrounds (a). Simulation of MCARI/OSAVI as function of C_{ab} and soil variation (b).

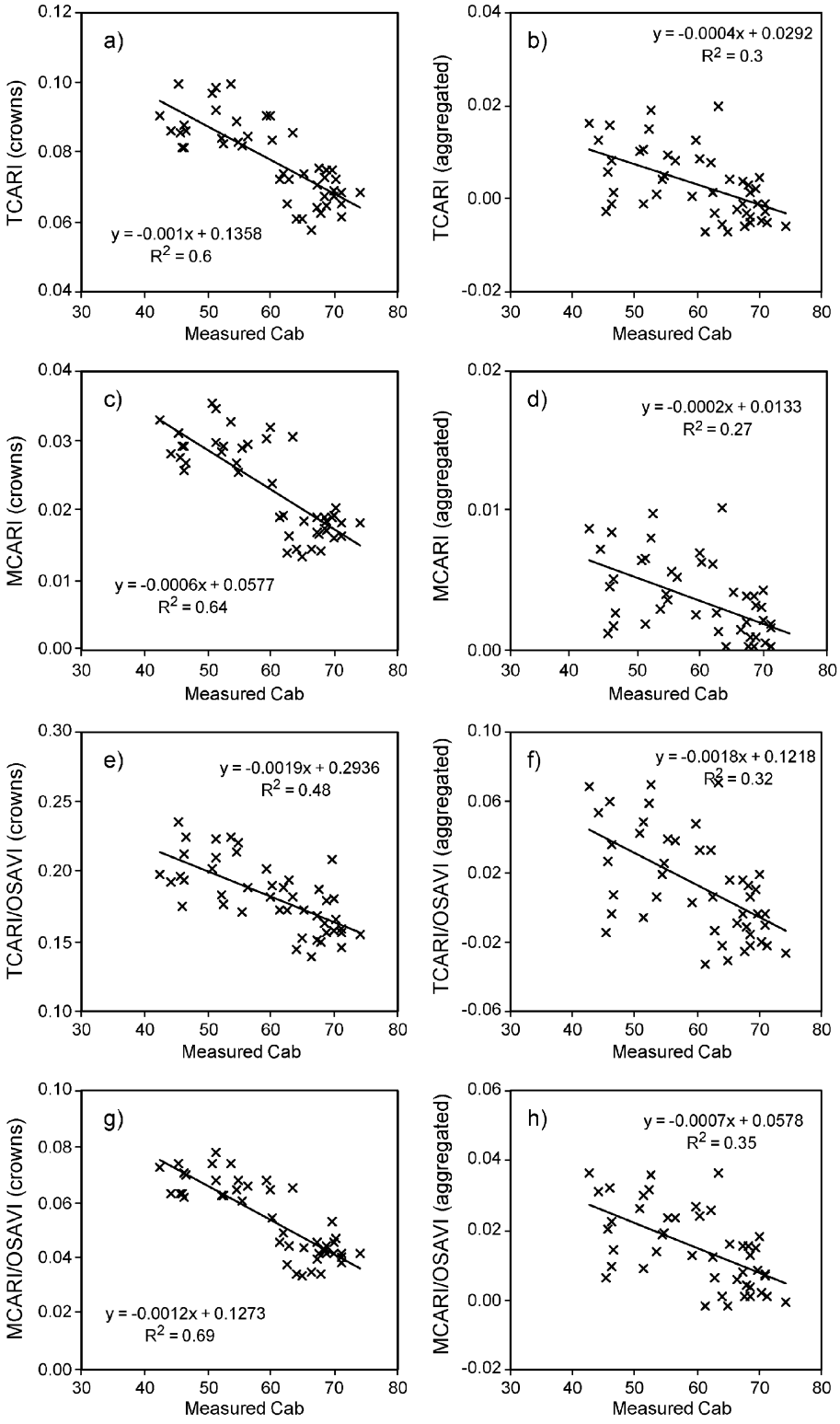

Fig. 11. Relationships between ground measured C_{ab} and TCARI, MCARI, TCARI//OSAVI, and MCARI/OSAVI indices calculated from imagery crown reflectance (a, c, e, g) and from imagery aggregated spectra (b, d, f, h), showing the large effects of scene components on the relationship between C_{ab} and the indices.

PECT-SAILH-FLIM with $T_\delta = 200$ trees/ha, $C_d = 7$ m, $C_h = 3$ m, $C_{LAI} = 1$, $C_\alpha = 0.6$, $\theta_s = 40°$, ρ_s from the adjacent soil pixel, and crown reflectance ρ_c from SAILH, illustrating the good agreement between the FLIM-simulated reflectance and the aggregated pixel from the image reflectance.

The effects of FLIM geometrical variables on MCARI/OSAVI were analysed to study their sensitivity on the simulated canopy reflectance (Fig. 9). Tree density, T_δ, crown diameter, C_d, and crown leaf area, C_{LAI}, were selected from among the other FLIM input variables due to their large effects on the simulated canopy reflectance. MCARI/OSAVI was simulated using PROSPECT-SAILH-FLIM with the input variables shown in Table 1, with T_δ ranging between 50 and 500 trees/ha, C_d between 1 and 9 m, and C_{LAI} between 0.5 and 3 (Fig. 9). FLIM simulation shows that larger effects on MCARI/OSAVI as function of tree density are found when C_{LAI} (Fig. 9a,b) and C_d increase (Fig. 9c,d). Small effects of T_δ on MCARI/OSAVI are found at low C_d (Fig. 9c). These simulations show that for the olive-tree geometries of the field sites used in this study, with low C_{LAI} (0.5–1.5) and large C_d (6–9 m) (Fig. 9a and d) the index MCARI/OSAVI is greatly affected by the tree density T_δ. This suggests that an accurate knowledge of the scene geometry and architecture should exist as prior information for accurate simulation using FLIM, and large errors are expected if these variables are not carefully considered.

PROSPECT-SAILH-FLIM models were used to generate a set of simulated spectra for different C_{ab} values and the three extreme soil backgrounds using the same set of input parameters previously described (Fig. 10a). The set of simulated spectra, which accounted for shadows and soil background through the FLIM model, enabled the study of the influence of C_{ab} and observed extreme range of soil reflectance on the MCARI/OSAVI index (Fig. 10b).

Single-ratio optical indices, combined indices, and the relationships derived from PROSPECT-SAILH for crowns, and PROSPECT-SAILH-FLIM for aggregated pixels, were then applied to the reflectance spectra derived from 1-m ROSIS imagery. Results for the relationships between estimated and ground-truth C_{ab} for the different modelling methods and *scaled-up* indices are described in the next section.

4. Results

Relationships between optical indices and ground measured C_{ab} when using 1-m ROSIS imagery targeting crowns (Table 2), yielded $r^2 = 0.6$ with TCARI (Fig. 11a), $r^2 = 0.64$ with MCARI (Fig. 11c), $r^2 = 0.48$ with TCARI/OSAVI combined index (Fig. 11e), and $r^2 = 0.69$ with MCARI/OSAVI (Fig. 11g). The combined index TCARI/OSAVI was more affected by the low LAI and soil background in this open canopy than MCARI/OSAVI. Single ratio index R_{750}/R_{710}, demonstrated in the literature to provide the best results in closed forest canopies, showed in this case expected sensitivity to influences of soil background, performing very poorly in open canopies even when crowns were targeted ($r^2 = 0.07$). This large effect of soil background on R_{750}/R_{710} index when targeting crowns was due to the low LAI of the *Olea europaea* L. crowns, with typical LAI values ranging between 0.5 and 1.5. Consistently, poorer results were obtained when indices were applied to the aggregated spectra (Fig. 3b) due to the large effects of soil and shadows on the indices, yielding $r^2 = 0.3$ (TCARI) (Fig. 11b), $r^2 = 0.27$ (MCARI) (Fig. 11d), $r^2 = 0.32$ (TCARI/OSAVI) (Fig. 11f), and $r^2 = 0.35$ (MCARI/OSAVI) (Fig. 11h). These results indicate that these indices, designed to minimize background effects and non-photosynthetic materials, are highly affected by direct soil background and shadow components in open canopies, requiring the appropriate modelling strategy when targeting crowns is not possible due to lower spatial resolution.

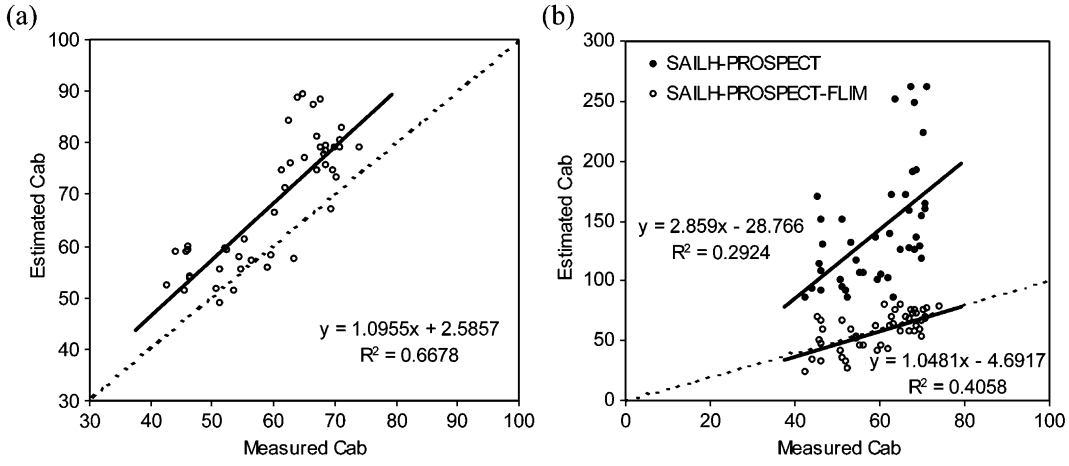

Fig. 12. Estimations of C_{ab} with MCARI/OSAVI predicting relationship and ROSIS crown reflectance spectra with PROSPECT-SAILH (a). Crown predictive relationship applied to aggregated pixels through PROSPECT-SAILH, improving the estimation when using PROSPECT-SAILH-FLIM (b).

The predictive relationship calculated for the MCARI/OSAVI index through PROSPECT-SAILH (Fig. 5c) using a gradient of soil backgrounds from bright to dark soil reflectance (Fig. 5a) and LAI = 0.5 yielded $r^2 = 0.67$ and RMSE = 10.9 μg/cm^2 (Fig. 12a) when applied to ROSIS pure-crown spectra. These results indicate that PROSPECT-SAILH simulation obtains reasonable results for C_{ab} estimation in open tree canopies when the spatial resolution is high and crowns can be targeted. Predictive relationships based on MCARI/OSAVI for LAI = 0.5 obtained the best RMSE, consistent with typical low LAI values in olive trees. Nevertheless, MCARI/OSAVI predictive relationships derived for higher LAI values showed an increase in RMSE, suggesting the high sensitivity of the index to low LAI values. MCARI/OSAVI relationships based on PROSPECT-SAILH derived for pure crowns were shown to be inaccurate when applied to ROSIS pixels with aggregated soil background and shadow scene components (Fig. 12b) yielding an $r^2 = 0.29$ and RMSE = 89.8 μg/cm^2. In this case of aggregated scene components, a relationship between MCARI/OSAVI and C_{ab} developed using PROSPECT-SAILH-FLIM to account for the scene components that were missing in the PROSPECT-SAILH simulation (Fig. 10b), significantly improved the estimation of C_{ab} yielding up to $r^2 = 0.41$ and decreasing RMSE down to 11.7 μg/cm^2 (Fig. 12b). These results demonstrate that crown-derived relationships with PROSPECT-SAILH between C_{ab} and optical indices such as MCARI/OSAVI cannot be readily applied to images of lower spatial resolution where crowns, shadows and soil components are aggregated within a pixel.

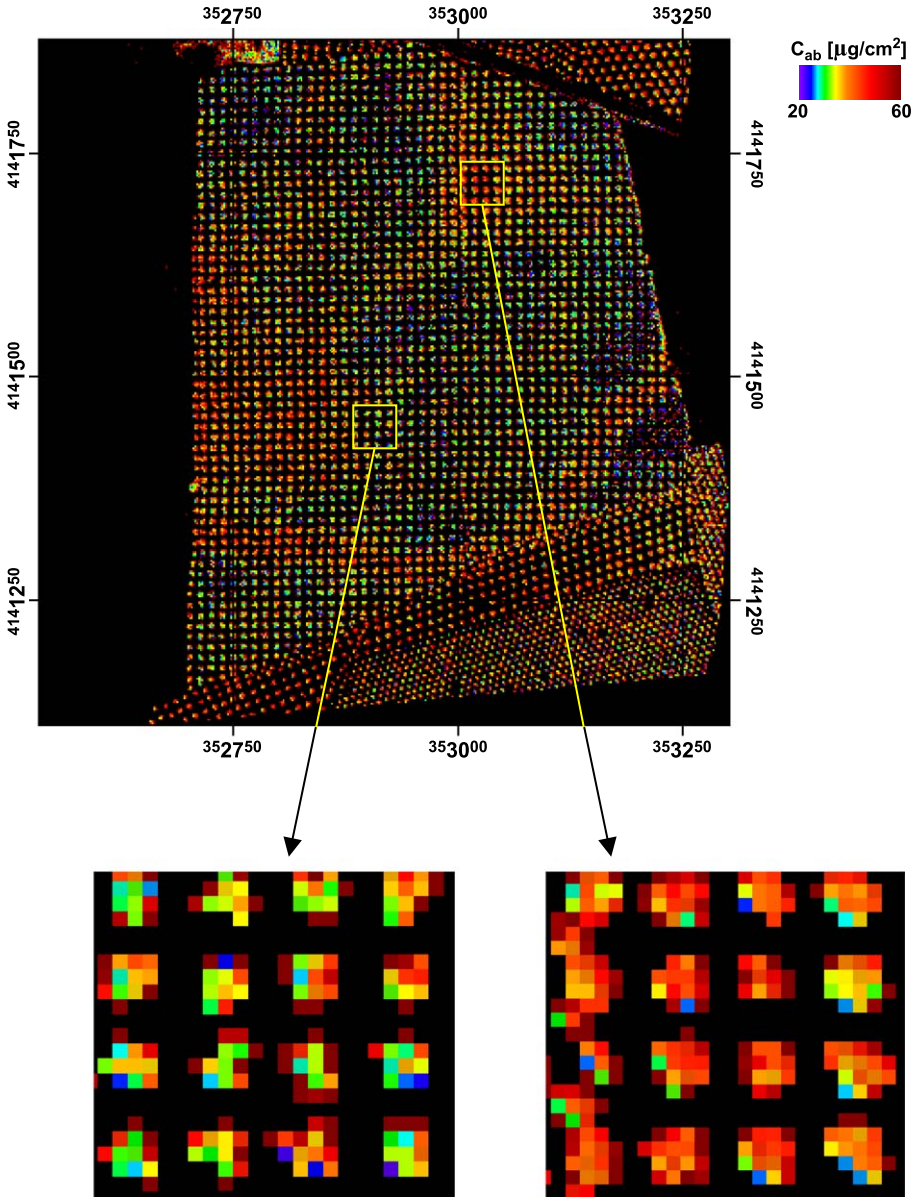

Fig. 13. Calculation of C_{ab} at the crown level by *scaling up* MCARI/OSAVI through PROSPECT-SAILH from 1-m ROSIS image.

In pixels with aggregated components, the use of a geometrical model, such as FLIM, to account for such background and shadow effects, including crown transparency, improved the estimation of C_{ab}, greatly reducing RMSE. FLIM simulations producing the best results overestimated crown diameter and was shown to be very sensitive to small variations of tree structural dimensions. The PROSPECT-SAILH-FLIM simulation resulted in a RMSE = 11.7 μg/cm^2 when building the MCARI/OSAVI relationship with $C_d = 7$ m, whereas a RMSE = 19.6 μg/cm^2 was obtained when using $C_d = 6.5$ m. This high sensitivity to small variations in crown dimensions poses a problem when applying this methodology to crop groves where variations in crown dimension are normally expected. Nevertheless, FLIM simulation results demonstrate that a radiative transfer model that accounts for shadow, soil and crown reflectance is required when pixel size aggregates all components. Calculation of C_{ab} using this method of *scaling up* MCARI/OSAVI through PROSPECT-SAILH (Fig. 13) shows the within-field variability of C_{ab} at the tree level at 1 m spatial resolution for the purpose of mapping stress condition and crop chlorosis detection.

5. Conclusions

Different methods have been explored in this research for stress detection through chlorophyll content estimation in open tree crop canopies. Hyperspectral ROSIS imagery acquired at 1 m spatial resolution from open crop fields of *Olea europaea* L. was analyzed in detail, supported by a field sampling campaign conducted for biochemical analysis of leaf C_{ab} on two fields of olive groves comprising irrigated and non-irrigated areas. Different radiative transfer model assumptions for open canopies along with optimum hyperspectral optical indices for C_{ab} estimation are discussed. The application of optical indices in discontinuous crop canopies such as *Olea europaea* L., where canopy structure plays an important role, and the effect of LAI, shadows and soil in the modelled reflectance have demonstrated the requirement for radiative transfer simulation methods for accurate estimates of biochemical constituents.

Relationships between optical indices and ground measured C_{ab} yielded reasonable results with 1-m ROSIS imagery when targeting crowns, obtaining the best results for MCARI/OSAVI, MCARI, and TCARI indices. The combined index TCARI/OSAVI was more affected by low LAI and soil background in this type of open canopy than MCARI/OSAVI. The single ratio red-edge index R_{750}/R_{710} that previously yielded good results in closed forest canopies showed in this case of an open canopy a large sensitivity to direct soil background effects, performing very poorly even when crowns were targeted, presumably due to the high canopy transmittance. As expected, these combined indices yielded poorer results for C_{ab} estimation when applied to aggregated spectra, due to the large effects of direct soil background and shadows on the optical indices. Results indicate that these combined indices are highly affected by soil background and shadow components in open canopies, requiring the use of open-canopy radiative transfer methods since canopy reflectance is then function of the three described components.

The *scaling-up* of the MCARI/OSAVI combined index through PROSPECT-SAILH provided fair results for C_{ab} estimation when crowns are targeted. This result indicates that PROSPECT-SAILH simulation can be used in open tree canopies when the spatial resolution is high and pure crown vegetation can be targeted. Nevertheless, PROSPECT-SAILH simulation of MCARI/OSAVI index derived for pure crowns was demonstrated to be inaccurate when applied to spectra comprised of soil background, shadow and crown components. As expected, PROSPECT-SAILH simulation was unable to account for soil and shadow components on the aggregated pixel. With aggregated scene components, the MCARI/OSAVI combined index was *scaled-up* through PROSPECT-SAILH-FLIM in order to account for all scene components. Crown-derived relationships with PROSPECT-SAILH between C_{ab} and optical indices such as MCARI/OSAVI could not be applied to spatially degraded imagery where crowns, shadows and soil components are aggregated, yielding large errors when estimating C_{ab}. The FLIM model was partially successful when accounting for background and shadow components, improving the estimation of C_{ab} by reducing the RMSE. Nevertheless, FLIM simulation overestimated the crown diameter and was shown to be very sensitive to small variations of tree structural dimensions.

This work demonstrates that a radiative transfer model that accounts for shadow, soil and crown reflectance is required when pixel size aggregates scene components, and that hyperspectral optical indices widely used in closed canopies are very sensitive to open-canopy characteristics. Further research should deal with the continuation of the proposed methods linking leaf-canopy models in open canopies with different crop architectures, tree dimensions, and plant densities to enable their application to high spatial resolution sensors unable to target crop crowns (i.e. 5 m spatial resolution imagery) and medium resolution data for global monitoring such as the MERIS sensor.

Acknowledgements

The authors gratefully acknowledge the HySens project support provided through the *Access to Research Infrastructures* EU Program. Financial support from the Spanish Ministry of Science and Technology (MCyT) for this project, support to A. Morales from project CAO 98-004, financial support to P.J. Zarco-Tejada under the MCyT ''Ramón y Cajal'' Program, as well by the Natural Sciences and Engineering Research Council of Canada to J. Miller are gratefully acknowledged. We thank S. Holzwarth, A. Müeller

and the rest of the DLR group at Oberpfaffenhofen for efficient airborne field campaigns, providing coordination with field data collection, and processing the datasets. V. Cachorro, A. de Frutos, A.J. Rodríguez, and M. Pérez are acknowledged for their support at different stages of the project.

References

Ben-Dor, E., & Levin, N. (2000). Determination of surface reflectance from raw hyperspectral data without simultaneous ground data measurements: A case study of the GER 63-channel sensor data acquired over Naan, Israel. *International Journal of Remote Sensing*, *21*, 2053–2074.

Carter, G. A. (1994). Ratios of leaf reflectances in narrow wavebands as indicators of plant stress. *International Journal of Remote Sensing*, *15*, 697–704.

Chen, Y., & Barak, P. (1982). Iron nutrition of plants in calcareous soils. *Advances in Agronomy*, *35*, 217–240.

Chova, M. M., Peña, F., del Campillo, M., Delgado, A., & Díaz, M. A. (2000). Efecto de la corección de la clorosis férrica en olivar con fosfato de hierro en los parámetros de calidad del aceite de oliva virgen. *Edafología*, 2–7.

Cordeiro, A. M., Alcántara, E., & Barranco, D. (1995). Differences in tolerance to iron deficiency among olive cultivar. In J. Abadia (Ed.), *Iron nutrition in soils and plants* (pp. 197–200). Netherlands: Kluwer Academic Publishing.

Daughtry, C. S. T., Walthall, C. L., Kim, M. S., Brown de Colstoun, E., & McMurtrey III, J. E. (2000). Estimating corn leaf chlorophyll concentration from leaf and canopy reflectance. *Remote Sensing of Environment*, *74*, 229–239.

Demarez, V., & Gastellu-Etchegorry, J. P. (2000). A modeling approach for studying forest chlorophyll content. *Remote Sensing of Environment*, *71*, 226–238.

Fernández-Escobar, R., Barranco, D., & Benlloch, M. (1993). Overcoming iron chlorosis in olive and peach trees using a low-pressure trunk-injection method. *Horticultural Science*, *28*, 192–194.

Fernández-Escobar, R., Moreno, R., & García-Creus, M. (1999). Seasonal changes of mineral nutrients in olive leaves during the alternate-bearing cycle. *Scientia Horticulturae*, *82*, 24–45.

Gitelson, A. A., & Merzlyak, M. N. (1996). Signature analysis of leaf reflectance spectra: Algorithm development for remote sensing of chlorophyll. *Journal of Plant Physiology*, *148*, 494–500.

Gitelson, A. A., & Merzlyak, M. N. (1997). Remote estimation of chlorophyll content in higher plant leaves. *International Journal of Remote Sensing*, *18*, 2691–2697.

Gutiérrez-Rosales, G., Garrido-Fernández, F. J., Galliardo-Guerrero, L., & Gandul-Rojas, B. (1992). Action of chlorophylls on the stability of virgin olive oil. *Journal of the American Oil Chemists' Society*, 69.

Haboudane, D., Miller, J. R., Tremblay, N., Zarco-Tejada, P. J., & Dextraze, L. (2002). Integrated narrow-band vegetation indices for prediction of crop chlorophyll content for application to precision agriculture. *Remote Sensing of Environment*, *81*, 416–426.

Harron, J. W. (2000), *Optical properties of phytoelements in conifers*, M. Sc. Thesis, Graduate Program in Earth and Space Science (p. 193) York University, Toronto, December, 2000.

Huete, A. R. (1988). A soil-adjusted vegetation index (SAVI). *Remote Sensing of Environment*, *25*, 295–309.

Jacquemoud, S. (1993). Inversion of the PROSPECT + SAIL canopy reflectance model from AVIRIS equivalent spectra: Theoretical study. *Remote Sensing of Environment*, *44*, 281–292.

Jacquemoud, S., Bacour, C., Poilve, H., & Frangi, J. P. (2000). Comparison of four radiative transfer models to simulate plant canopies reflectance-direct and inverse mode. *Remote Sensing of Environment*, *74*, 471–481.

Jacquemoud, S., & Baret, F. (1990). Prospect: A model for leaf optical properties spectra. *Remote Sensing of Environment*, *34*, 75–91.

Jacquemoud, S., Baret, F., Andrieu, B., Danson, F. M., & Jaggard, K. (1995). Extraction of vegetation biophysical parameters by inversion of the PROSPECT + SAIL models on sugar beet canopy reflectance data. Application to TM and AVIRIS sensors. *Remote Sensing of Environment*, *52*, 163–172.

Jolley, V. D., & Brown, J. C. (1994). Genetically controlled uptake and use of iron by plants. In J. A. Manthey, D. E. Crowley, & D. G. Luster (Eds.), *Biochemistry of metal micronutrients in the rhizosphere* (pp. 251–266). Boca Raton: Lewis.

Kim, M. S., Daughtry, C. S. T., Chappelle, E. W., McMurtrey III, J. E., & Walthall, C. L. (1994). The use of high spectral resolution bands for estimating absorbed photosynthetically active radiation (Apar). In *6th Symp. on Physical Measurements and Signatures in Remote Sensing, Jan. 17–21, 1994, Val D'Isere, France* (pp. 299–306). Paris/Toulouse (France): ISPRS Commission VII WG I, CNES.

Mariscal, M., Orgaz, F., & Villalobos, F. J. (2000). Modelling and measurement of radiation interception by olive canopies. *Agricultural and Forest Meteorology*, *100*, 183–197.

Marschner, H., Romheld, V., & Kissel, M. (1986). Different strategies in higher plants in mobilization and uptake of iron. *Journal of Plant Nutrition*, *9*, 695–713.

Miller, J. R., Hare, E. W., & Wu, J. (1990). Quantitative characterization of the vegetation red edge reflectance: An inverted-Gaussian model. *International Journal of Remote Sensing*, *11*, 1755–1773.

Rock, B. N., Hoshizaki, T., & Miller, J. R. (1988). Comparison of In Situ and airborne spectral measurements of the blue shift associated with forest decline. *Remote Sensing of Environment*, *24*, 109–127.

Rondeaux, G., Steven, M., & Baret, F. (1996). Optimization of soil-adjusted vegetation indices. *Remote Sensing of Environment*, *55*, 95–107.

Rosema, A., Verhoef, W., Noorbergen, H., & Borgesius, J. J. (1992). A new forest light interaction model in support of forest monitoring. *Remote Sensing of Environment*, *42*, 23–41.

Schulze, E. D., De Vries, W., & Hauhs, M. (1989). Critical loads for nitrogen deposition in forest ecosystems. *Water, Air and Soil Pollution*, *48*, 451–456.

Tagliavini, M., & Rombolà, A. D. (2001). Iron deficiency and chlorosis in orchard and vineyard ecosystems. *European Journal of Agronomy*, *15*, 71–92.

Verhoef, W. (1984). Light scattering by leaf layers with application to canopy reflectance modeling: The SAIL model. *Remote Sensing of Environment*, *16*, 125–141.

Villalobos, F. J., Orgaz, F., & Mateos, L. (1995). Non-destructive measurement of leaf area in olive (*Olea europaea L.*) trees using a gap inversion method. *Agricultural and Forest Meteorology*, *73*, 29–42.

Vogelmann, J. E., Rock, B. N., & Moss, D. M. (1993). Red edge spectral measurements from sugar maple leaves. *International Journal of Remote Sensing*, *14*, 1563–1575.

Wallace, A. (1991). Rational approaches to control of iron deficiency other than plant breeding and choice of resistant cultivars. *Plant and Soil*, *130*, 281–288.

Wellburn, A. R. (1994). The spectral determination of chlorophylls *a* and *b*, as well as total carotenoids using various solvents with spectrophotometers of different resolutions. *Journal of Plant Physiology*, *144*, 307–313.

Zarco-Tejada, P. J., Miller, J. R., Noland, T. L., Mohammed, G. H., & Sampson, P. H. (2001). Scaling-up and model inversion methods with narrow-band optical indices for chlorophyll content estimation in closed forest canopies with hyperspectral data. *IEEE Transactions on Geoscience and Remote Sensing*, *39*(7), 1491–1507.